Thermal Degradation Analysis of Mamoncillo (*Melicoccus bijugatus*) Waste: Thermal Behaviors, Kinetics, and Thermodynamics

Análisis de degradación térmica de residuos de mamoncillo (*Melicoccus bijugatus*): comportamiento térmico, cinético y termodinámico

Andrés Felipe Rojas-González[1] and Francisco Javier Velasco-Sarria[2]

ABSTRACT

This research studied the thermal conversion characteristics, kinetics, and thermodynamics of *mamoncillo* peels and seeds using non-isothermal thermogravimetric analysis. Kinetic analysis was performed using the Kissinger-Akahira-Sunose, Flynn-Wall-Ozawa, Starink, and Friedman methods. The reaction kinetic models were obtained by means of the master-plots method for 18 different empirical reaction models, calculating the enthalpy, Gibbs free energy, and entropy as thermodynamics parameters. It was found that the average activation energy for *mamoncillo* peels and seeds was 238,71 and 197,60 kJ/mol, respectively. The frequency factor was found to be between 10^9 and 10^{31} s^{-1} for *mamoncillo* peels and between 10^9 and 10^{34} s^{-1} for *mamoncillo* seeds. The average values of ΔH and ΔG were also found to be 233,83 and 192,81 kJ/mol and 164,84 and 162,10 kJ/mol for *mamoncillo* peels and seeds, respectively. The reaction kinetic models regarding the thermal decomposition of *mamoncillo* peels were found to be described by the contracting cylinder (R2) and third-order (F3) models, while those for *mamoncillo* seeds can be described by the second-order (F2) and contracting sphere (R3) models. It was concluded that the pyrolysis process of *mamoncillo* waste can be described by a complex reaction mechanism, and that these wastes have thermal properties with the potential to produce bioenergy.

Keywords: tkinetic models, mamoncillo wastes, pyrolysis, thermodynamic analysis

RESUMEN

En este estudio se investigaron las características de conversión térmica, cinéticas y termodinámicas de las semillas y cáscaras de mamoncillo utilizando análisis termogravimétrico no isotérmico. El análisis cinético se realizó empleando los métodos de Kissinger-Akahira-Sunose, Flynn-Wall-Ozawa, Starink y Friedman. Los modelos cinéticos de reacción se obtuvieron mediante el método de gráficas maestras para 18 modelos de reacción empíricos diferentes, y, como parámetros termodinámicos, se calcularon la entalpía, la energía libre de Gibbs y la entropía. Se encontró que la energía de activación promedio para las cáscaras y las semillas de mamoncillo fue de 238,71 y 197,60 kJ/mol respectivamente. El factor de frecuencia estuvo entre 10^9 y 10^{31} s^{-1} para las cáscaras de mamoncillo y entre 10^9 y 10^{34} s^{-1} para las semillas de mamoncillo. También se encontró que el valor promedio de ΔH y ΔG estaba entre 233,83 y 192,81 kJ/mol y 164,84 y 162,10 kJ/mol para las cáscaras y las semillas respectivamente. Se encontró que los modelos cinéticos de reacción para la descomposición térmica de cáscaras de mamoncillo se pueden describir mediante los modelos cilindro de contracción (R2) y de tercer orden (F3), mientras los de las semillas se pueden describir por medio de los modelos de segundo orden (F2) y esfera de contracción (R3). Se concluyó que el proceso de pirólisis de los residuos de mamoncillo se puede describir utilizando un mecanismo de reacción complejo, y que estos residuos presentan propiedades térmicas con potencial para producir bioenergía.

Palabras clave: túneles, método de elementos finitos, Mohr-Coulomb, elástico-elastoplástico

Introduction

The growing global demand for electricity, thermal energy, and fuels, the deterioration of the environment, and the depletion of fossil fuel reserves have led to the search for alternative energy sources, mainly of lignocellulosic origin. One of these alternatives is lignocellulosic biomass waste (*i.e.*, agro-industrial waste), which is characterized by being a low-cost, highly available, renewable, and sustainable material (Pacheco *et al.*, 2022). Agro-industrial waste includes fruit byproducts, which mainly consist of peels and seeds. Fruit byproducts are obtained from direct consumption and/ or processing to obtain juices, jellies, wines, pulps, *etc.* (Lam *et al.*, 2016). This biomass is composed of cellulose (32-45%), hemicellulose (19-25%), lignin (14-26%), extractives, and ash (Rony *et al.*, 2019).

---

[1] PhD in Engineering – Chemical Engineering, Universidad del Valle, Colombia. Affiliation: Associate professor, Universidad Nacional de Colombia, Chemical Engineering Department, Colombia. E-mail: anfrojasgo@unal.edu.co

[2] PhD in Engineering, Universidad del Valle, Colombia. Affiliation: Technical director of the Fuels Combustion Laboratory, Universidad del Valle, Colombia. E-mail: francisco.velasco@correounivalle.edu.co

One of the fruits produced and directly consumed in the intertropical zone of America is *mamoncillo*, also known as *mamón* or *quenepa* (Calderón *et al.*, 2021). This fruit generates peels and seeds as waste, which represent 65% of the whole fruit. *Mamoncillo* seeds have been studied to determine their polyphenol content and antioxidant capacity and as a source of starch (Moo-Huchin *et al.*, 2020). These seeds have been used for the extraction of dyes with applications in fabric dyeing (Vejar *et al.*, 2016), and studies have been conducted on their total flavonoids content, total phenolic compounds and, antioxidant activity have been evaluated (Can-Cauich *et al.*, 2017).

Lignocellulosic biomass can be converted to solid, liquid, and gaseous products, which are employed to obtain fuels or value-added products (Kumar *et al.*, 2020). These products can be obtained through several technological routes, which can be categorized as *thermochemical*, *biochemical*, and *physicochemical* (Bridgwater, 2012). Thermochemical conversion processes can be further subdivided into combustion, gasification, liquefaction, and pyrolysis. They are used to transform biomasses into bio-oil, gaseous fuel, and biochar (Emiola-Sadiq *et al.*, 2021). Pyrolysis is the simplest thermochemical conversion process to produce biochar, bio-oils, and syngas, which has industrial and ecological importance and plays an important role in the development of bioenergy systems (Bensidhom *et al.*, 2021). This conversion process is considered to be efficient and low-cost, and it is classified as slow, fast, and flash pyrolysis depending on the heating rate and residence time (Kan *et al.*, 2012). Fast and flash pyrolysis are used to transform biomass into bio-oil, while slow pyrolysis transforms biomass into gaseous fuel and charcoal (Gogoi *et al.*, 2018).

To better understand pyrolysis and its operation, it is essential to know the kinetic and thermodynamic parameters involved, as well as the thermal characteristics of the biomass (Yang *et al.*, 2019; Pawar *et al.*, 2021). Thermogravimetric analysis (TGA) is a powerful technique to understand the biomass pyrolysis process. This technique gives detailed information about reaction mechanisms, stability, reactivity, thermodynamic parameters, and decomposition kinetics (Emiola-Sadiq *et al.*, 2021). TGA can be categorized as isothermal or non-isothermal. Non-isothermal analysis is carried out for linear heating rates, which involves heating the biomass from room temperature to a desired temperature at a desired constant heating rate (Mishra and Bhaske, 2014). The data obtained from non-isothermal TGA can be handled using isoconversional (model-free methods) or model-fitting methods (Gogoi *et al.*, 2018). The most commonly employed model-free techniques are the Kissinger-Akahira-Sunose (KAS), Flynn-Wall-Ozawa (FWO), Starink, and Friedman methods. These are used to calculate kinetic parameters as recommended by the Kinetics Committee of the International Confederation for Thermal Analysis and Calorimetry (ICTAC) (Vyazovkin *et al.*, 2011). To predict mechanisms or kinetic models, the ICTAC recommends the Coats-Redfern integral method

and master-plots associated with Criado method (Santos *et al.*, 2020).

This study presents the thermal, kinetic, and thermodynamic analysis of *mamoncillo* (*Melicoccus bijugatus*) waste (peels and seeds) by means of pyrolysis using non-isothermal thermogravimetry at three heating rates (10, 20, and 40 ˚C/min). The kinetic parameters (activation energy, E_a; pre-exponential factor, A_a) of *mamoncillo* waste were determined via three integral isoconversional methods (KAS, FWO, and Starink) and a differential isoconversional method (Friedman). The mechanism or kinetic model for the thermal degradation reaction of the *mamoncillo* waste was established using the master-plots method and 18 different reaction mechanisms. Other thermodynamic parameters were determined, such as enthalpy (ΔH), Gibbs free energy (ΔG), and entropy (ΔS).

Methods

Materials

Mamoncillo peels and seeds were collected from fruits and vegetables stores in the city of Manizales, Colombia. These wastes were reduced in size to dimensions of less than 1 cm. Then, they were dried at 45 ˚C until they reached constant weight in order to avoid the loss of substances with low molecular weight. Afterwards, they were reduced in size using a disc mill to obtain a powder of less than 250 μm (-60 mesh). Finally, the powdered samples were stored in plastic bags and placed in a desiccator to prevent moisture absorption.

Feedstock characterization

The powdered *mamoncillo* wastes were characterized for proximate, ultimate, and higher heating value (HHV) analysis. These tests were carried out in triplicate, and the standard deviation of the data was determined. Proximate, moisture, ash, and volatile matter analyses were carried out according to the ASTM-E871-82 (2019), ASTM E872-82 (2019), and ASTM E1577-11 standards. The fixed carbon content was determined by difference. The elemental composition of carbon, hydrogen, and nitrogen was quantified using a LECO-CHN628 analyzer, while the amount of sulfur was obtained using a LECO-S632 analyzer. The oxygen content was determined by difference, and the HHV was obtained using an SDACM3100 bomb calorimeter.

Thermogravimetric analysis

Thermal analysis experiments were performed in a TA-Instrument-Q600 simultaneous TGA-DSC thermogravimetric analyzer. Pyrolysis was carried out at three heating rates (10, 20, and 40 ˚C/min), heating between room temperature and 900 ˚C in an inert atmosphere (nitrogen) and with a gas flow of 100 ml/min. The experiments were carried out at a high nitrogen flow rate to eliminate some secondary reactions (Chen *et al.*, 2017). To reduce the limiting steps

of the degradation reaction due to mass and heat transfer, a sample size of 15-16 mg was maintained. Meanwhile, to reduce diffusion limitations, the samples were maintained at a particle size of less than 250 µm. This analysis was carried out in duplicate. The TGA results were used to obtain kinetic and thermodynamic parameters.

Kinetic analysis

In this work, the kinetic parameters and the reaction mechanism for the thermal degradation of *mamoncillo* peels and seeds were determined. The thermal decomposition of lignocellulosic biomass is a heterogeneous process because the biomass components undergo thermochemical reactions in the solid state, with very complex reaction mechanisms (Santos *et al.*, 2020). Therefore, determining the pyrolysis kinetics of biomass requires the use of different reaction kinetic models.

The so-called *model-free methods* are based on determining E_a without knowing the reaction's kinetic model (Chen *et al.*, 2017; Liu *et al.*, 2020). They are also known as *isoconversional methods* because i) E_a is obtained as a function of conversion, and ii), as an isoconversial principle, at a particular conversion, the reaction rate for the thermal decomposition of biomass is function of temperature (non-isothermal analysis) (Singh *et al.*, 2020a). Among the most used isoconversional methods to calculate kinetic parameters are the KAS, FWO, and Starink integral methods, in addition to the Friedman differential method (Singh *et al.*, 2020a). The Equations of these methods are presented below:

$$ln\left(\frac{\beta}{T_\alpha^2}\right) = ln\left[\frac{A_a R}{E_a g(\alpha)}\right] - \frac{E_a}{RT_\alpha} \tag{1}$$

FWO method (Santos *et al.*, 2020):

$$ln(\beta) = ln\left[\frac{A_a R}{E_a g(\alpha)}\right] - 5,331 - 1,052\left(\frac{E_a}{RT_\alpha}\right) \tag{2}$$

Starink method (Singh *et al.*, 2020a):

$$ln\left(\frac{\beta}{T_\alpha^{1,92}}\right) = C - 1.008\left(\frac{E_a}{RT_\alpha}\right) \tag{3}$$

Friedman method (Gogoi *et al.*, 2018):

$$ln\left(\beta\frac{d\alpha}{dT}\right) = ln\left[A_a f(\alpha)\right] - \frac{E_a}{RT_\alpha} \tag{4}$$

where α is the fractional conversion; E_a, A_a, and T_a are the activation energy, pre-exponential factor, and absolute temperature for a value α, respectively; β is the heating rate; R is the universal gas constant (8,314 J/kmol.K); $g(\alpha)$ is a function that describes a reaction model in its integral form; $f(\alpha)$ is a function that describes a reaction model in its differential form; and C is a constant. Table 1 presents the algebraic expression of 18 different reaction models, which are a function of $f(\alpha)$ and $g(\alpha)$.

Here, $f(0,5)$ and $g(0,5)$ are functions that describe various reaction models in differential and integral form, respectively. They are evaluated at a fractional conversion of 0,5. $T_{0,5}$ is the absolute temperature at a conversion value of 0,5. The $Z(\alpha)$ master-plot consists of theoretical curves from different reaction kinetic models for solid-state degradation reactions, which are independent of the kinetic parameters (Wang *et al.*, 2019; Singh *et al.*, 2021). In these curves, the integral and differential forms of the reaction models are combined. These curves are used to identify the most appropriate theoretical kinetic model that describes an experimental reaction process.

To predict the mechanisms or kinetic model of thermal degradation reactions, the recommendations given by the ICTAC (Vyazovkin *et al.*, 2011) were followed, which involve using the master-plots method in association with the Criado method (Santos *et al.*, 2020). To this effect, the following Equation was used (Gogoi *et al.*, 2018; Santos *et al.*, 2020; Aboulkas *et al.*, 2010):

$$\frac{Z(\alpha)}{Z(0,5)} = \frac{f(\alpha)g(\alpha)}{f(0.5)g(0,5)} = \left(\frac{T_\alpha}{T_{0,5}}\right)^2\left[\frac{(d\alpha/dt)_\alpha}{(d\alpha/dt)_{0,5}}\right] \tag{5}$$

The theoretical master-plots were constructed by plotting for each kinetic model, while the experimental master-plot was obtained by plotting with experimental data (Santos *et al.*, 2020). Both terms of Equation (5) were plotted as a function of fractional conversion. The coincidence of a theoretical master-plot with the experimental one indicates that the thermal degradation of biomass is carried out by means of the reaction kinetic model given by the theoretical master curve (Aboulkas *et al.*, 2010).

$$\frac{f(\alpha)g(\alpha)}{f(0,5)g(0,5)} \qquad \left(\frac{T_\alpha}{T_{0,5}}\right)^2\left[\frac{(d\alpha/dt)_\alpha}{(d\alpha/dt)_{0,5}}\right]$$

In this research, the four isoconversional methods (KAS, FWO, Starink, and Friedman) were used to determine E_a. A_a was calculated by means of Equation (6), while the reaction mechanism or kinetic model ($f(\alpha)$) of the thermal decomposition for *mamoncillo* waste was obtained using master-plots.

Thermodynamic parameters

The thermodynamic analysis of the mamoncillo waste was carried out by calculating the enthalpy (ΔH), Gibbs free

Table 1. Thermal degradation kinetic models in the solid state

Reaction Models	$f(\alpha)$	$g(\alpha)$
Nucleation models		
Power law (P2)	$2\alpha^{1/2}$	$\alpha^{1/2}$
Power law (P3)	$3\alpha^{2/3}$	$\alpha^{1/3}$
Power law (P2/3)	$2/3\alpha^{-1/2}$	$\alpha^{3/2}$
Power law (P4)	$4\alpha^{3/4}$	$\alpha^{1/4}$
Avarami-Erofeev (A1)	$(3/2)(1-\alpha)$ $[-\ln(1-\alpha)]^{1/3}$	$[-\ln(1-\alpha)]^{2/3}$
Avarami-Erofeev (A2)	$2(1-\alpha)[-\ln(1-\alpha)]^{1/2}$	$[-\ln(1-\alpha)]^{1/2}$
Avarami-Erofeev (A3)	$3(1-\alpha)[-\ln(1-\alpha)]^{2/3}$	$[-\ln(1-\alpha)]^{1/3}$
Avarami-Erofeev (A4)	$4(1-\alpha)[-\ln(1-\alpha)]^{3/4}$	$[-\ln(1-\alpha)]^{1/4}$
Diffusion models		
One-dimensional diffusion (D1)	$1/(2\alpha)$	α^2
Two dimensional (D2) - (Valensi model)	$-[1/\ln(1-\alpha)]$	$[(1-\alpha)\ln(1-\alpha)]+\alpha$
Diffusion control (D3) - (Jander model)	$[3(1-\alpha)^{2/3}]/[2(1-(1-\alpha)^{1/3})]$	$[1-(1-\alpha)^{1/3}]^2$
Diffusion control (D4) - (Ginstling-Brounshtein model)	$(3/2)[((1-\alpha)^{-1/3}-1)]^{-1}$	$1-(2/3)\alpha-(1-\alpha)^{2/3}$
Reaction order models		
Zero order (F0)	1	α
First order (F1) – (Mampel Model)	$(1-\alpha)$	$-\ln(1-\alpha)$
Second order (F2)	$(1-\alpha)^2$	$[1/(1-\alpha)]-1$
Third order (F3)	$(1-\alpha)^3$	$(1/2)[(1-\alpha)^{-2}-1]$
Geometrical contraction models		
Contracting cylinder (R2)	$2(1-\alpha)^{1/2}$	$1-(1-\alpha)^{1/2}$
Contracting sphere (R3)	$3(1-\alpha)^{2/3}$	$1-(1-\alpha)^{1/3}$

Source: Emiola-Sadiq *et al*. (2021), Mishra and Bhaske (2014), Vyazovkin *et al*. (2011)

energy (ΔG), and entropy (ΔS) via the KAS, FWO, Starink, and Friedman methods. These parameters, together with E_a and A_a, allow better understanding the pyrolysis process of biomass. This analysis is fundamental to establishing the feasibility and efficiency of pyrolysis, as well as for the calculation of energy consumption or requirements (Singh *et al*., 2020a). A, ΔH, ΔG, and ΔS, are given by the following Equations (Singh *et al*., 2021; Raza *et al*., 2022):

$$A_a = \frac{\beta E_a}{RT_m^2} e^{\left(\frac{E_a}{RT_m}\right)} \tag{6}$$

$$\Delta H = E_a - RT_m \tag{7}$$

$$\Delta G = E_a + RT_m \ln\left(\frac{k_B T_m}{h A_a}\right) \tag{8}$$

$$\Delta S = \frac{\Delta H - \Delta G}{T_m} \tag{9}$$

where E_a is the activation energy obtained via different isoconversional methods; β denotes the heating rates; R is the universal gas constant (8,314 J/kmol.K); T_m is the peak temperature in the DTG curve; k_b is the Boltzmann constant (1,3819 x 10^{-23} J/K); and h is the Planck constant (6,6269 x 10^{-34} J.s) (Kumar *et al*., 2020; Santos *et al*., 2020).

Results and discussion

Waste characterization

The results obtained for the proximate analysis on a dry basis, the ultimate analysis on a dry ash free basis, the atomic ratios, and the HHV of *mamoncillo* wastes are shown in Table 2. Note that the total moisture, ash, and fixed carbon content are higher in the peels than in the seeds. *Mamoncillo* peels have four times more ash content than the seeds. The peels can cause issues related to slags, corrosion, or clogging in the equipment (Chen *et al*., 2018). Additionally, a high ash content can cause poor heat generation and reduced energy conversion (Singh *et al*., 2020a). The high volatile matter contents in the seeds should facilitate ignition at low temperatures and benefit the formation of gaseous and liquid products during the pyrolysis process (Santos *et al*., 2020). These wastes have the same fixed carbon content, and they are in the range required for efficient burning, which is between 15 and 25% (Santos *et al*., 2020). The empirical formulas for the peels and seeds, as obtained from the ultimate analysis, are $C_{20}H_{29,5}O_{13,7}N_{0,20}S_{0,04}$ and $C_{20}H_{29,4}O_{13,9}N_{0,14}S_{0,03}$, respectively. Both wastes have the same empirical formula. These similar results lead to similar values for the the atomic ratios H/C and O/C and the HHV. However, the little difference in HHV is due to the fact that the *mamoncillo* peels have a higher ash content (Rojas and Flórez, 2019).

Table 2. Proximate and ultimate analysis of *mamoncillo* waste

	Peels	*Seeds*
Proximate analysis, %		
Total moisture	66,99±2,23	59,54±1,78
Ash*	5,23±0,51	1,33±0,12
Volatile mater*	77,12±1,75	83,54±1,92
Fixed carbon*	17,65±0,83	15,13±0,89
Ultimate analysis, %**		
Carbon – C	48,73±1,07	48,55±1,15
Hydrogen – H	6,04±0,11	6,00±0,13
Oxygen – O	44,37±0,92	44,89±1,01
Nitrogen – N	0,58±0,02	0,29±0,01
Sulfur – S	0,39±0,01	0,18±0,01
Atomic ratio H/C	1,49±0,07	1,40±0,09
Atomic ratio O/C	0,68±0,03	0,69±0,02
High heating value-HHV, MJ/kg*	18,08±0,79	19,09±0,94

*Dry basis. **Dry ash free basis.
Source: Authors

Thermogravimetric analysis

Figure 1 shows the TG/DTG curves for the peels (Figure 1a) and the seeds (Figure 1b) at three heating rates. Note that thermal decomposition of *mamoncillo* waste can be described using three main zones (Santos *et al.*, 2020). The first zone indicates the drying of wastes, and it is called the *passive zone*, where the total moisture is removed (Wang *et al.*, 2019; Singh *et al.*, 2021). This zone is between 30 and 170 °C for peels and 30 and 190 °C for seeds. In the second zone, the *main active pyrolysis zone* (Emiola-Sadiq *et al.*, 2021), the elimination of volatile matter takes place, which happens between 170 and 650 °C for peels and 190 and 590 °C for seeds. In the last zone, there is char formation, with temperatures of >650 and >590 °C for peels and seeds, respectively. The peak temperatures for the three different heating rates are 303,22, 314,50, and 326,20 °C for peels, and 291,49, 303,17, and 315,56 °C for seeds. These results indicate that *mamoncillo* seeds are pyrolytically more reactive than *mamoncillo* peels.

Kinetic analysis

The kinetic parameters corresponding to the pyrolysis of *mamoncillo* waste were evaluated by calculating E_a and A_a via the KAS, FWO, Starink, and Friedman isoconversional methods. To obtain the kinetic properties, only the second zone in the DTG curve was considered, as it is characterized by the highest mass loss has the fraction that is considered to be pyrolysable (Mehmood *et al.*, 2017).
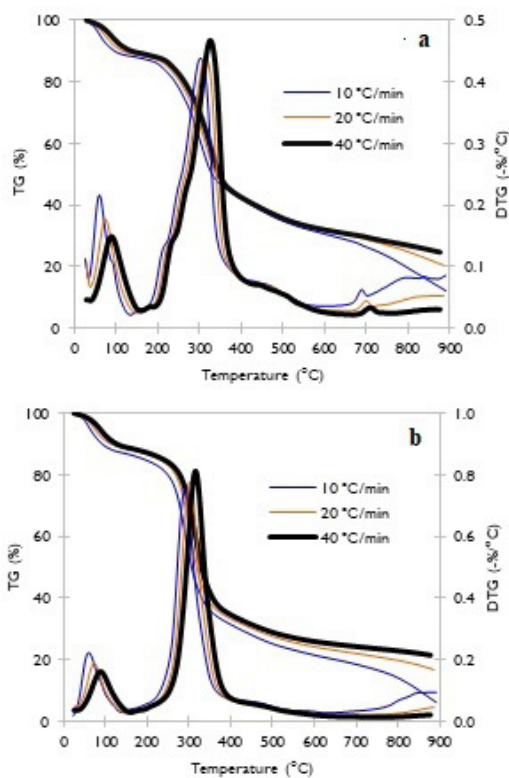

Figure 1. TG/DTG curves at different heating rates for a) *mamoncillo* peels and b) *mamoncillo* seeds
Source: Authors

Figures 2a and 2b show the variations of E_a with conversion (α=0,05-0,80) as estimated via the isoconversional methods for *mamoncillo* peels and seeds. Regarding mamoncillo peels, it was found that E_a varies with conversion ranges of 132,94-365,40, 134,20-357,21, 132,21-362,92 and 152,24-578,27 kJ/mol for the KAS, FWO, Starink, and Friedman methods, respectively. As for the seeds, E_a varies with conversion ranges of 120,07-389,62, 122,03-380,32, 119,44-386,94, and 135,13-491,09 kJ/mol. The average E_a for the peels are 240,15, 237,36, 238,63, and 296,84 kJ/mol for these methods. For the *mamoncillo* seeds, the average E_a are 198,22, 197,49, 197,10, and 228,25 kJ/mol. It was also found that, for the KAS, FWO, and Starink methods, the activation energy deviation from the average E_a was between 29 and 31% for the peels and from 33 to 35% for the seeds. For the Friedman method, these deviations were 47 and 42% for peels and seeds, respectively. These results indicate that the integral methods were more accurate than the differential method (Vyazovkin *et al.*, 2011).

During the pyrolysis of *mamoncillo* waste, E_a showed little variations with regard to the KAS, FWO, and Starink methods. For the peels, the average values obtained were 240,15, 237,36, and 238,63 kJ/mol, respectively. For the seeds, these values were 198,22, 197,49, and 197,10 kJ/mol. Meanwhile, the Friedman method reported significant variations, with values of 296,84 and 228,25 kJ/mol for the peels and seeds, respectively. These results indicate that *mamoncillo* seeds are more reactive than *mamoncillo* peels during the pyrolysis process (Singh *et al.*, 2020a). Moreover, Figure 2 shows that conversions of up to 0,20 and low E_a values (184 kJ/mol for peels and 161 kJ/mol for seeds) are needed to break the weaker bonds between molecules and remove light components. This indicates the start of the pyrolysis reaction (Pawar *et al.*, 2021). For conversions between 0,20 and 0,70, the value of E_a increases to 270 kJ/mol for peels and 201 kJ/mol for seeds. This may be mainly due to cellulose as well as hemicellulose pyrolysis (Santos *et al.*, 2020). For conversions greater than 0,70, a higher E_a was found, which is due to lignin pyrolysis (Pawar *et al.*, 2021).

As mentioned earlier, model-free methods can generally be split into two categories: differential and integral. These are used for estimating kinetic parameters (pre-exponential factor, activation energy, and reaction order) (Vyazovkin *et al.*, 2011). The activation energy may show differences depending on the method used for calculation. These differences are due to the inherent and unavoidable inaccuracy and imprecision of differential methods. Therefore, they can sometimes exhibit numerical instability when compared to integral methods; when the reaction heat varies noticeably with the temperature program and when they are applied to differential data, their accuracy can be limited due to the difficulty in determining the baseline (Vyazovkin *et al.*, 2011; Cai *et al.*, 2018). The Friedman method is the most general isoconversional differential technique, and it requires derivative conversion data, which leads it to be numerically unstable and sensitive to noise

(Cai *et al.*, 2018). In fact, in this work, the Friedman method showed a higher average E_a than KAS, FWO, and Starink for both *mamoncillo* wastes. This behavior can also be explained by the fact that the Friedman method normally depends on the instantaneous rate of biomass conversion without any pre-assumptions, which it is not possible in integral methods (Pawar *et al.*, 2021). The authors used this method for the sake of comparison, but they do not recommend using it.
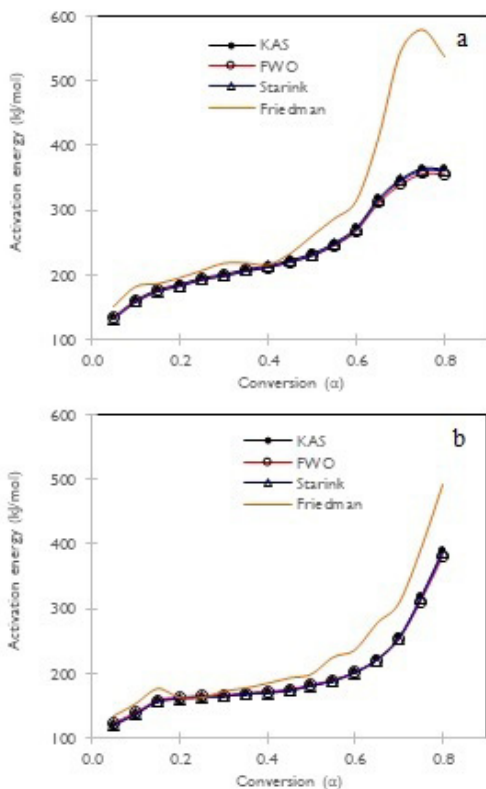

Figure 2. Activation energy at different conversions using the KAS, FWO, Starink and Friedman methods for. a) *Mamoncillo* peels, b) *mamoncillo* seeds.
Source: Authors

Table 3 presents the variations in A_a with conversion (α=0,05-0,80) at 10 °C/min as estimated via isoconversional methods for *mamoncillo* waste. This factor, also called the *frequency factor*, measures the frequency of active collision that occurs between the reactant molecules. It is used to explain the chemistry of the pyrolysis reaction, and it serves to optimize the experimental conditions of pyrolytic processes (Santos *et al.*, 2020). It is known that, for A_a <10^9 s^{-1}, only surface reactions are taking place, while A_a >10^9 s^{-1} indicates that i) there is a complex reaction, which does not depend on the contact surface area; ii) a high collision of molecules is required; and iii) a high E_a is needed for biomass pyrolysis (Kaur *et al.*, 2017). In our study, the A_a values calculated via the KAS, FWO, and Starink methods were found to be between 10^9 and 10^{31} s^{-1} for peels and between 10^9 and 10^{34} s^{-1} for seeds. It was found that A_a varies with conversion as E_a changes, *i.e.*, A_a increases when the conversion is higher.

It was also found that A_a decreases with the increase in heating rate. This indicates that, at low conversions (<0,20), the reactivity of the thermal decomposition of *mamoncillo* wastes is low, with the highest values at high conversion (Singh *et al.*, 2020a).

Reaction kinetic models

We predicted the reaction model during the pyrolysis of mamoncillo waste using 18 reaction kinetic models (solid-state mechanisms) with the corresponding experimental and theoretical master-plot curves. The experimental and theoretical curves at 10 °C/min are presented in Figure 3.

Table 3. Pre-exponential factor (A_a) for *mamoncillo* wastes *vs.* the degree of conversion at 10 °C/min

	A_a, s^{-1} - Peels			A_a, s^{-1} - Seeds		
α	KAS	FWO	Starink	KAS	FWO	Starink
0,05	8,96x10^9	1,18x10^{10}	7,65x10^9	9,68x10^9	1,49x10^9	8,43x10^9
0,10	2,83x10^{12}	2,98x10^{12}	2,32x10^{12}	4,06x10^{10}	5,80x10^{10}	3,45x10^{10}
0,15	1,00x10^{14}	9,25x10^{13}	7,98x10^{13}	3,11x10^{12}	3,76x10^{12}	2,56x10^{12}
0,20	5,60x10^{14}	4,95x10^{14}	4,42x10^{14}	7,89x10^{12}	9,40x10^{12}	6,46x10^{12}
0,25	5,25x10^{15}	4,30x10^{15}	4,07x10^{15}	1,43x10^{13}	1,69x10^{13}	1,17x10^{13}
0,30	1,65x10^{16}	1,32x10^{16}	1,27x10^{16}	1,85x10^{13}	2,20x10^{13}	1,51x10^{13}
0,35	9,13 x10^{16}	6,86x10^{16}	6,95x10^{16}	3,50x10^{13}	4,09x10^{13}	3,69x10^{13}
0,40	2,91x10^{17}	2,12x10^{17}	2,20x10^{17}	6,25x10^{13}	7,20x10^{13}	5,05x10^{13}
0,45	1,92x10^{18}	1,30x10^{18}	1,43x10^{18}	1,33x10^{14}	1,49x10^{14}	1,07x10^{14}
0,50	1,61x10^{19}	1,00x10^{19}	1,18x10^{19}	6,62x10^{14}	6,98x10^{14}	5,25x10^{14}
0,55	5,70x10^{20}	3,03x10^{20}	4,06x10^{20}	3,62x10^{15}	3,56x10^{15}	2,84x10^{15}
0,60	8,86x10^{22}	3,75x10^{22}	6,09x10^{22}	5,97x10^{16}	5,21x10^{16}	4,59x10^{16}
0,65	1,25x10^{27}	3,39x10^{26}	7,99x10^{26}	4,56x10^{18}	3,28x10^{18}	3,39x10^{18}
0,70	8,03x10^{29}	1,64x10^{29}	4,87x10^{29}	6,37x10^{21}	3,29x10^{21}	4,48x10^{21}
0,75	2,80x10^{31}	5,10x10^{30}	1,66x10^{31}	4,85x10^{27}	1,33x10^{27}	3,07x10^{27}
0,80	2,33x10^{31}	4,63x10^{30}	1,39x10^{31}	2,72x10^{34}	3,66x10^{33}	1,53x10^{34}

Source: Authors

Regarding the *mamoncillo* peels, it can be seen (Figure 3a) that, for conversions from 0,05 to 0,50, the experimental curve almost overlaps the R2 model or the contracting cylinder model, and, for conversion ranges between 0,50 and 0,80 the experimental curve is close to the F3 model or the third-order reaction model. It can be concluded that the decomposition of *mamoncillo* peels in each conversion range (0,05-0,50 and 0,50-0,80) can be described by a single reaction model. Meanwhile, regarding the *mamoncillo* seeds (Figure 3b), note that, for conversions between 0,05 and 0,50, the experimental curve is close to the F2 model or the second-order reaction model, and, for conversion ranges of 0,50-0,80, the experimental curve almost overlaps the R3 model or the contracting sphere model. This indicates that the pyrolysis of *mamoncillo* seeds can be described by a complex reaction mechanism.

Thermodynamic parameters

The thermodynamic parameters ΔH, ΔG, and ΔS involved in the thermal decomposition of mamoncillo wastes were calculated using the activation energy obtained via the KAS, FWO, Starink, and Friedman methods. The values of ΔH, ΔG, and ΔS were calculated using Equations (7) to (9). The changes in ΔH, ΔG and ΔS with the conversion value at 10°C/min are reported in Tables 4-9, respectively. ΔH is the minimum energy required by the biomass to form products during pyrolysis (Singh *et al.*, 2021; Kaur *et al.*, 2017). Thereupon, ΔH evaluates the total energy consumed in the conversion of *mamoncillo* waste into products (Santos *et al.*, 2020). ΔG represents the increase in the system's total energy for the formation of activated complexes (Maia and Morais, 2016), and it can be used to determine whether the reactions are spontaneous. A negative ΔG value indicates the occurrence of spontaneous reactions, while a positive value denotes a nonspontaneous reaction (Chen *et al.*, 2023). Meanwhile, ΔS is associated with the measure of randomness or disorder of energy and matter in a system, as well as to the formation of new chemical compounds (Kumar *et al.*, 2020).
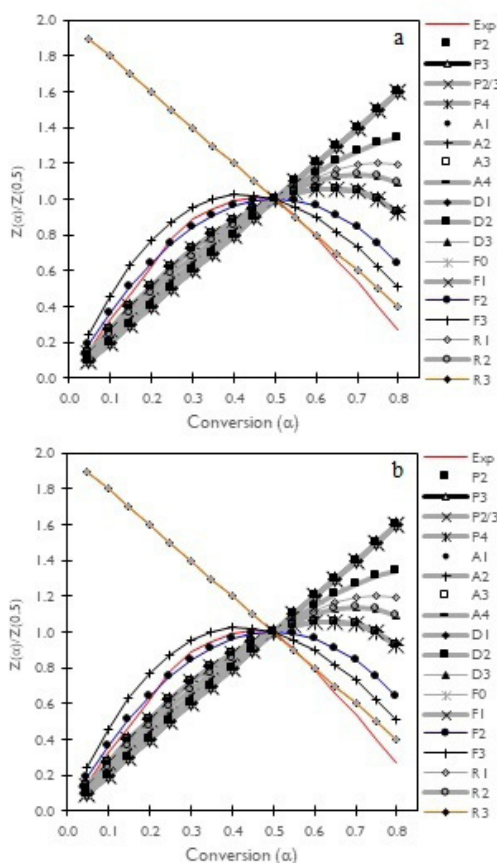

Figure 3. Master-plots for different kinetic models and experimental data at 10 °C/min for a) mamoncillo peels and b) *mamoncillo* seeds
Source: Authors

In Tables 4 and 5, it can be seen that, for both wastes, i) ΔH increases with conversion for all methods except for Friedman; ii) the average values are similar for the KAS, FWO, and Starink methods; iii) the H values for the Friedman method are higher than those of KAS, FWO, and Starink; iv) the ΔH values for *mamoncillo* seeds are lower than those reported for *mamoncillo* peels; and v) all ΔH values are positive.

Positive ΔH values indicate that the thermal degradation of *mamoncillo* wastes took place via endothermic reactions. This means that an external source of heat is required to transform biomass into gas, oil, and charcoal during the pyrolysis process (Chen *et al.*, 2017; Kumar *et al.*, 2020). It was found that the difference between the values of E_a and ΔH at each conversion level is less than 5 kJ/mol. This small difference indicates the formation of low-energy activated complexes in the product-forming potential barrier (Santos *et al.*, 2020). Therefore, the pyrolysis of *mamoncillo* wastes for energy generation is viable (Kumar *et al.*, 2020; Santos *et al.*, 2020). Moreover, for the *mamoncillo* peels, the average ΔH values at three heating rates (10, 20, and 40°C/min) for the KAS, FWO, Starink, and Friedman methods were 235,27 ± 0,10, 232,47 ± 0,10, 233,74 ± 0,10, and 291,95 ± 0,10 kJ/mol, respectively. For *mamoncillo* seeds, these values were 193,42 ± 0,10, 192,70 ± 0,10, 192,30 ± 0,10, and 223,46 ± 0,10 kJ/mol, respectively. These results show that the effect of the heating rate on ΔH is negligible. Similar results were reported for banana leaves (Singh *et al.*, 2020a) and acai seeds (Santos *et al.*, 2020). It can be seen that *mamoncillo* seeds consume less total energy than *mamoncillo* peels during their conversion into products.

Table 4. ΔH variations with conversion at 10 °C/min for *mamoncillo* peels for the KAS, FWO, Starink, and Friedman methods

ΔH, kJ/mol				
α	KAS	FWO	Starink	Friedman
0,05	128,14	129,41	127,42	147,45
0,10	154,84	155,08	153,92	178,07
0,15	171,45	171,09	170,40	182,49
0,20	179,49	178,92	178,39	191,49
0,25	189,95	189,02	188,77	202,62
0,30	195,32	194,26	194,10	214,00
0.,35	203,32	201,99	202,04	214,42
0,40	208,76	207,26	207,44	211,76
0,45	217,60	215,77	216,22	228,82
0,50	227,59	225,36	226,13	256,15
0,55	244,34	241,37	242,75	282,66
0,60	268,09	264,04	266,32	310,44
0,65	313,15	306,98	311,02	406,55
0,70	343,68	336,18	341.,2	539,85
0,75	360,48	352,42	357,99	573,48
0,80	359,61	351,96	357,15	532,53
Average	**235,36**	**232,57**	**233,84**	**292,05**

Source: Authors

The variations in ΔG with the conversion level for *mamoncillo* peels and seeds as obtained via the KAS, FWO, Starink, and Friedman methods are shown in Tables 6 and 7. The average ΔG values for *mamoncillo* waste are in the range between 162 and 164 kJ/mol. The ΔG values are similar for both wastes. However, the average ΔG values the peels were slightly higher than those obtained for the seeds, which means that, for thermal decomposition, peels require more heat. Similar results have been reported for the pyrolysis of agricultural residues (Chen *et al.*, 2017). In addition, ΔG was found to decrease with conversions of 0,05-0,80, implying that the energy of the reaction system decreased when the pyrolysis started (Yuan *et al.*, 2017). It was also found that, for both wastes, ΔG is positive, which indicates that the thermal decomposition reaction is nonspontaneous. Therefore, this reaction requires energy consumption for the chemical bonds to break. This result suggests that the reactivity of the thermal degradation was low and that the pyrolysis process requires an external energy source to obtain the activated complex (Chen *et al.*, 2017).

Table 5. ΔH variations with conversion at 10 °C/min for *mamoncillo* peels for the KAS, FWO, Starink, and Friedman methods

ΔH, kJ/mol				
α	KAS	FWO	Starink	Friedman
0,05	115,37	117,33	114,75	130,43
0,10	132,30	133,91	131,56	149,20
0,15	152,03	152,90	151,14	172,37
0,20	156,27	157,08	155,36	158,44
0,25	158,99	159,76	158,06	158,40
0,30	160,17	160,96	159,24	168,43
0,35	163,08	163,79	163,32	173,13
0,40	165,72	166,37	164,75	180,41
0,45	169,16	169,71	168,16	188,74
0,50	176,51	176,76	175,46	194,48
0,55	184,29	184,22	183,18	220,71
0,60	197,14	196,52	195,93	232,08
0,65	217,05	215,54	215,69	273,03
0,70	250,39	247,34	248,77	303,86
0,75	312,94	306,94	310,82	386,87
0,80	384,93	375,62	382,25	486,36
Average	**193,52**	**192,80**	**192,40**	**223,56**

Source: Authors

Table 6. ΔG variations with conversion at 10 °C/min for *mamoncillo* peels for the KAS, FWO, Starink, and Friedman methods

ΔG, kJ/mol				
α	KAS	FWO	Starink	Friedman
0,05	167,45	167,40	167,47	349,76
0,10	166,57	166,56	166,60	379,58
0,15	166,09	166,10	166,12	382,14
0,20	165,88	165,90	165,91	390,54
0,25	165,62	165,64	165,64	401,05
0,30	165,49	165,51	165,51	411,65
0,35	165,30	165,33	165,33	411,21
0,40	165,17	165,21	165,20	407,75
0,45	164,98	165,02	165,01	424,66
0,50	164,77	164,82	164,80	452,14
0,55	164,44	164,49	164,47	478,84
0,60	164,00	164,07	164,03	506,77
0,65	163,27	163,36	163,30	604,22
0,70	162,83	162,93	162,86	740,10
0,75	162,60	162,71	162,63	776,34
0,80	162,61	162,71	162,62	736,82
Average	**164,82**	**164,86**	**164,85**	**490,85**

Source: Authors

Tables 8 and 9 present the variations in ΔS with the conversion level for *mamoncillo* peels and seeds as obtained via the KAS, FWO, Starink, and Friedman methods. ΔS is negative at conversion of up to 0,10 for the peels, and the seeds exhibit negative values up to a fractional conversion of 0,30. Low ΔS values indicate that these wastes undergo small physical and chemical charges during thermal degradation, transitioning to a new condition close to thermodynamic equilibrium (Dhyani *et al.*, 2017), increasing the pyrolysis reaction time (Singh *et al.*, 2020b). For high ΔS values, the reactivity is high, the reaction time decreases, and the process is far from thermodynamic equilibrium (Singh *et al.*, 2021; Mallick *et al.*, 2018). Here, ΔS increased when the fractional conversion increased for the KAS, FWO, and Starink methods and both wastes, implying that the pyrolysis was far from reaching equilibrium. The ΔS values calculated via the Friedman method are all negative for *mamoncillo* waste. ΔS followed similar trend as ΔH and E_a, which increased with the increasing fractional conversion. This can be attributed to the fact that the reaction rate increased for the 0,05-0,80 conversions (Singh *et al.*, 2021).

Table 7. ΔG variations with conversion at 10 ˚C/min for *mamoncillo* peels for the KAS, FWO, Starink, and Friedman methods

ΔG, kJ/mol				
α	KAS	FWO	Starink	Friedman
0,05	164,23	164,15	164,25	332,46
0,10	163,61	163,55	163,63	347,15
0,15	162,98	162,95	163,00	367,27
0,20	162,85	162,83	162,88	350,56
0,25	162,77	162,75	162,80	349,12
0,30	162,74	162,71	162,76	358,58
0,35	162,66	162,64	162,65	362,74
0,40	162,58	162,56	162,61	369,80
0,45	162,49	162,47	162,52	378,17
0,50	162,29	162,29	162,32	383,90
0,55	162,10	162,10	162,12	411,22
0,60	161,79	161,80	161,82	423,15
0,65	161,35	161,38	161,37	465,50
0,70	160,69	160,74	160,72	497,33
0,75	159,66	159,75	159,69	581,91
0,80	158,70	158,81	158,73	684,78
Average	**162,09**	**162,09**	**162,12**	**416,48**

Source: Authors

The knowledge of thermogravimetric, kinetic, and thermodynamic parameters is fundamental in determining the feasibility and efficiency of the pyrolysis process, designing pyrolyzers, determining the energy balance, and calculating the energy consumption or requirements (Kumar *et al.*, 2020, Singh *et al.*, 2020a). These parameters can be used to determine the optimal operating conditions to obtain a specific pyrolysis product (bio-oil, biochar, and syngas) (Li *et al.*, 2023) from *mamoncillo* wastes. Therefore, this study can contribute to understanding *mamoncillo* waste pyrolysis and its future applications. For example, it was found that these wastes have an ignition temperature (Figure 1) between 210 ˚C (peels) and 250 ˚C (seeds), as well as high volatile matter contents (between 77 and 84% on a dry basis). This indicates that the pyrolysis of these wastes can produce more bio-oil than biochar and syngas (Nawaz *et al.*, 2021). On the other hand, by controlling the operating conditions, it is possible to produce a higher proportion of biochar than bio-oil and syngas, or a higher proportion of syngas than bio-oil and biochar. These wastes have different applications. Bio-oil can be used as solid biofuel for cooking purposes and domestic heating, or as a solvent for extracting important chemical compounds. Biochar can be used as a soil and water conditioner (it is a good biosorbent), as a solid fuel for cooking purposes and domestic heating, or as

a supercapacitor (Nawaz *et al.*, 2021; Li *et al.*, 2023). On the other hand, condensable gases or synthesis gas (syngas) can be used as a biofuel for combustion engines or boilers (Nawaz *et al.*, 2021).

Table 8. ΔS variations with conversion at 10 ˚C/min for *mamoncillo* peels for the KAS, FWO, Starink, and Friedman methods

ΔS, J/mol K				
α	KAS	FWO	Starink	Friedman
0,05	-68,19	-65,91	-69,50	-351,02
0,10	-20,34	-19,92	-22,00	-349,63
0,15	9,30	8,65	7,43	-346,40
0,20	23,62	22,59	21,65	-345,35
0,25	42,22	40,56	40,12	-344,27
0,30	51,76	49,87	49,59	-342,92
0,35	65,97	63,60	63,70	-341,43
0,40	75,62	72,96	73,28	-340,04
0,45	91,29	88,05	88,84	-339,79
0,50	108,99	105,04	106,41	-340,05
0,55	138,63	133,38	135,82	-340,36
0,60	180,59	173,45	177,46	-340,64
0,65	260,04	249,18	256,30	-342,95
0,70	313,78	300,58	309,62	-347,43
0,75	343,31	329,15	338,95	-351,95
0,80	341,78	328,34	337,46	-354,44

Source: Authors

Conclusions

The kinetics involved in the thermal degradation of mamoncillo peels and seeds was determined by means of TGA experiments at three heating rates (10, 20, and 40 ˚C/min). The E_a and the frequency factor were calculated using four isoconversional methods (KAS, FWO, Starink, and Friedman). The E_a was found to be slightly constant in the 0,15-0,50 conversion range, but E_a increased with increases between 0,50 to 0,80, suggesting that the studied pyrolysis was a multistep process. The frequency factor values were found to be between 10^9 and 10^{34} s^{-1}, which indicates that thermal degradation occurred under complex reactions. The optimal kinetic models for the pyrolysis of *mamoncillo* peels were R2, or the contracting cylinder model, in the conversion range of 0,05-0,50 and the F3, or the third-order reaction model, in the conversion range of 0,50-0,80. Meanwhile, for *mamoncillo* seeds, the optimal kinetic models were F2, or the second-order reaction model, in the conversion range of 0,05-0,50 and R3, or the contracting sphere model, in the conversion range of 0,50-0,80. This indicates that the pyrolysis of *mamoncillo* wastes can be characterized by a complex reaction mechanism. The results obtained for the

thermodynamic parameters (ΔH, ΔG, and ΔS) suggest that *mamoncillo* waste has properties associated with a potential use as a bioenergy source. The positive ΔH, positive ΔG, and negative ΔS values confirm that the studied pyrolysis process is endothermic and nonspontaneous.

Table 9. ΔS variations with conversion at 10 °C/min for *mamoncillo* peels for the KAS, FWO, Starink, and Friedman methods

ΔS, J/mol K				
α	KAS	FWO	Starink	Friedman
0,05	-86,52	-82,91	-87,67	-357,80
0,10	-55,45	-52,50	-56,80	-350,58
0,15	-19,39	-17,80	-21,00	-345,16
0,20	-11,64	-10,18	-13,31	-340,25
0,25	-6,69	-5,30	-8,39	-337,79
0,30	-4,54	-3,11	-6,25	-336,77
0,35	0,75	2,05	1,19	-335,80
0,40	5,56	6,74	3,79	-335,41
0,45	11,82	12,81	10,01	-335,49
0,50	25,18	25,63	23,27	-335,46
0,55	39,30	39,18	37,29	-337,39
0,60	62,62	61,49	60,42	-338,39
0,65	98,66	95,92	96,19	-340,87
0,70	158,87	153,37	155,94	-342,65
0,75	271,46	260,68	267,66	-345,44
0,80	400,65	383,98	395,86	-351,41

Source: Authors

Acknowledgements

CRedit author statement

Andrés Felipe Rojas-González conceived the idea and did the background research, collected the data, developed the workflow, performed the assessment, supervised the research, and provided critical feedback. Francisco Javier Velasco-Sarria helped to do the background research, collected literature data, conducted the formal analysis, collected experimental data, and provided critical feedback. All authors contributed to writing the manuscript and approved its definitive version for publication.

Conflicts of interest

The authors declare that they have no conflict of interest that could influence the contents of this manuscript.

References

Aboulkas, A., El harfi, K., and El Bouadili, A. (2010). Thermal degradation behaviors of polyethylene and polypropylene. Part 1: Pyrolysis kinetics and mechanisms. *Energy Conversion Management*, *51*, 1363-1369. https://doi.org/10.1016/j.enconman.2009.12.017

Bensidhom, G., Trabelsi, B. H., Mahmood, M. A., and Ceylan, S. (2021). Insights into pyrolite feedstock potential of date palm industry wastes: Kinetic study and product characterization. *Fuel*, *285*, 119096. https://doi.org/10.1016/j.fuel.2021.119096

Bridgwater, A. V. (2012). Review of fast pyrolysis of biomass and product upgrading. *Biomass and Bioenergy*, *38*, 68-94. https://doi.org/10.1016/j.biombioe.2011.01.048

Calderón, J. C., Sachdev, H., Thepanondh, S., and Quintanilla, Y. A. (2021). Morphological and physico-chemical characterization of fruit of *melicoccus bijugatus jacq*. *Bangladesh Journal Botanic*, *50*(2), 387-394. https://doi.org/10.3329/bjb.v50i2.54096

Cai, J., Xu, D., Dong, Z., Yu, X., Yang, Y., and Banks, S. W. (2018). Processing thermogravimetric analysis data for isoconversional kinetic analysis of lignocellulosic biomass pyrolysis: Case study of corn stalk. *Renewable and Sustainable Energy Reviews*, *82*, 2705-2715. https://dx.doi.org/10.1016/j.rser.2017.09.113

Can-Cauich, C. A., Sauri-Duch, E., Betancur-Ancona, D., Chel-Guerrero, L., González-Aguilar, G. A., Cuevas-Glory, L. F., Pérez-Pacheco, E., and Moo-Huchin, V. M. (2017). Tropical fruit peel powders as functional ingredients: Evaluation of their bioactive compounds and antioxidant activity. *Journal of Functional Foods*, *37*, 501-506. https://doi.org/doi:10.1016/j.jff.2017.08.028

Chen, D., Shuang, E., and Liu, L. (2018). Analysis of pyrolysis characteristics and kinetics of sweet sorghum bagasse and cotton stalk. *Journal of Thermal Analysis and Calorimetry*, *131*, 1899-1909. https://doi.org/10.1007/s10973-017-6585-9

Chen, J., Wang, Y., Lang, X., Ren, X., and Fan, S. (2017). Evaluation of agricultural residues pyrolysis under non-isothermal conditions: Thermal behaviors, kinetics, and thermodynamics. *Bioresource Technology*, *241*, 340-348. https://doi.org/10.1016/j.biortech.2017.05.036

Chen, X., Cai, D., Yang, Y., Sun, Y., Wang, B., Yao, Z., Jin, M., Liu, J., Reinmoller, M., Badshah, S. L., and Magdziarz, A. (2023). Pyrolysis kinetics of bio-based polyurethane: Evaluating the kinetic parameters, thermodynamic parameters, and complementary product gas analysis using TG/FTIR and TG/GC-MS. *Renewable Energy*, *205*, 490-498. https://doi.org/10.1016/j.renene.2023.01.078

Dhyani, V., Kumar, L., and Bhaskar, T. (2017). Thermal decomposition kinetics of sorghum straw via thermogravimetric analysis. *Bioresource Technology, 245*, 1122-1129. https://doi.org/10.1016/j.biortech.2017.08.189

Emiola-Sadiq, T., Zhang, L., and Dalai, A.K. (2021). Thermal and kinetic studies on biomass degradation via thermogravimetric analysis: A combination of model-fitting and model-free approach. *ACS Omega, 6*, 22233-22247. https://doi.org/10.1021acsomega.1c02937

Gogoi, M., Konwar, K., Bhuyan, N., Borah, R. C., Kalita, A. C., Nath, H. P., and Saikia, N. (2018). Assessments of pyrolysis kinetics and mechanisms of biomass residues using thermogravimetry. _Bioresource Technology Reports_, _44_, 0-49. https://doi.org/10.1016/j.biteb.2018.08.016

Kan, T., Strezov, V., and Evans, T.J. (2012). Lignocellulosic biomass pyrolysis: A review of product properties and effects of pyrolysis parameters. _Renewable and Sustainable Energy Reviews_, _57_, 1126-1140. https://doi.org/10.1016/j.rser.2015.12.185

Kaur, R., Gera, P., Jha, M. K., and Bhaskar, T. (2017). Pyrolysis kinetics and thermodynamic parameters of castor (_Ricinus communis_) residue using thermogravimetric analysis. _Bioresource Technology_, _250_, 422-428. https://doi.org/10.1016/j.biortech.2017.11.077

Kumar, M., Shukla, S. K., Upadhyay, S. N., and Mishra, P. K. (2020). Analysis of thermal degradation of banana (_Musa balbisiana_) trunk biomass waste using iso-conversional models. _Bioresource Technology_, _310_, 123393, https://doi.org/10.1016/j.biortech.2020.123393

Lam, S. S., Liew, R. K., Lim, X. Y., Ani, F. N., and Jusoh, A. (2016). Fruit waste as feedstock for pyrolysis technique. _International Biodeterioration & Biodegradation_, _113_, 325-333. https://doi.org/10.1016/j.ibiod.2016.02.021

Li, Y., Wan, Y., Chai, M., Li, Ch, Nishu, L., Yellezuome, D., and Liu, R. (2023). Pyrolysis kinetics and thermodynamic parameters of bamboo residues and its three main components using thermogravimetric analysis. _Biomass and Bioenergy_, _170_, 106705. https://doi.org/10.1016/j.biombioe.2023.106705

Liu, H., Chen, B., and Wang, C. (2020). Pyrolysis kinetics study of biomass waste using Shuffled Complex Evaluation algorithm. _Fuel Processing Technology._, _208_, 106509. https://doi.org/10.1016/j.fuproc.2020.106509

Maia, A. D., and Morais, L. C. (2016). Kinetic parameters of red pepper waste as biomass to solid biofuel. _Bioresource Technology_, _204_, 157-163. https://doi.org/10.1016/j.biortech.2015.12.055

Mallick, D., Poddar, M. K., Mahanta, P., and Moholkar, V. S. (2018). Discernment of synergism in pyrolysis of biomass blends using thermogravimetric analysis. _Bioresource Technology_, _261_, 294-305. https://doi.org/10.1016/j.biortech.2018.04.011

Mehmood, M. A., Ye, G., Luo, H., Liu, C., Malik, S., Afzal, I., Xu, J., and Ahmad, M. S. (2017). Pyrolysis, and kinetic analyses of Camel grass (_Cymbopogon schoenanthus_) for bioenergy. _Bioresource Technology_, _228_, 18-24. https://doi.org/10.1016/j.biortech.2016.12.096

Mishra, G., and Bhasker, T. (2014). Non isothermal model-free kinetics for pyrolysis of rice straw. _Bioresource Technology_, _169_, 614-621. https://doi.org/10.1016/j.biortech.2014.07.045

Moo-Huchin, V. M., Ac-Chim, D.M., Chim-Chi, Y. A., Ríos-Soberanis, C. R., Ramos, G., Yee-Madeira, H. T., Ortiz-Fernández, A., Estrada-León, R. J., and Pérez-Pacheco, E. (2020). Huaya (_Melicoccus bijugatus_) seed four as a new source of starch: Physicochemical, morphological, thermal, and functional characterization. _Journal of Food Measurement and Characterization, 14_, 3299-3309. https://doi.org/10.1007/s11694-020-00573-3

Nawaz, A., Misha, R. K., Sabbarwal, S., and Kumar P. (2021). Studies of physicochemical characterization and pyrolysis behavior of low-value waste biomass using thermogravimetric analyzer: Evaluation of kinetic and thermodynamic parameters. _Bioresource Technology Reports, 16_, 100858. https://doi.org/10.1016/j.biteb.2021.100858

Pacheco, J. I., Lucca, F. A., Goncalves, W. D., Chacón, G., and Sousa, V. (2022). Influence of biomass waste from agro-industries on obtaining energetic gases assisted by chronoamperometric process. _International Journal Hydrogen Energy_, _47_(2), 735-746. https://doi.org/10.1016/j.ijhydene.2021.10.045

Pawar, A., Panwar, N. L., Jain, S., Jain, N. K., and Gupta, T. (2021). Thermal degradation of coconut husk waste biomass under non-isothermal condition. _Biomass Conversion and Biorefinery, 13_, 7613-7622. https://doi.org/10.1007/s13399-021-01657-w

Raza, M., Abu-Jdayil, B., Al-Marzouqi, A.H., and Inayat, A. (2022). Kinetic and thermodynamic analyses of date palm surface fibers pyrolysis using Coats-Redfern method. _Renewable Energy,_ 163, 67-77. https://doi.org/10.1016/j.renene.2021.10.065

Rojas, A. F., and Flórez, C. (2019). Valorización de residuos de frutas para combustión y pirólisis. _Revista Politécnica, 15_(28), 42-53. https://doi.org/10.33571/rpolitec.v15n28a4

Rony, A. H., Koug, L., Lu, W., Dejam, M., Adidharma, H., Gasem, K. A. M., Zheng, Y., Norton, U., and Fan, M. (2019). Kinetics, thermodynamics, and physical characterization of corn stover (Zea mays) for solar biomass pyrolysis potential analysis. _Bioresource Technology, 284_, 466-473. https://doi.org/10.1016/j.biortech.2019.03.049

Santos, V. O., Queiroz, L. S., Araujo, R. O., Ribeiro, F. C. P., Guimaraes, M. N., Costa, C. E. F., Chaar, J. S., and Souza, L. K. C. (2020). Pyrolysis of acai seed biomass Kinetics and thermodynamic parameters using thermogravimetric analysis. _Bioresource Technology Reports, 12_, 100553. https://doi.org/10.1016/j.biteb.2020.100553

Singh, R. K., Patil, T., Pandey, D., and Sawarkar, A. N. (2020a). Pyrolysis of banana leaves biomass: Physico-chemical characterization, thermal decomposition behavior, kinetic and thermodynamic analyses. _Bioresource Technology_, _310_, 123464. https://doi.org/10.1016/j.biortech.2020.123464

Singh, R. K., Patil, T., and Sawarkar, A. N. (2020b). Pyrolysis of garlic husk biomass: Physico-chemical characterization, thermodynamic and kinetic analyses. _Bioresource Technology Reports, 12_, 100558. https://doi.org/10.1016/j.biteb.2020.100558

Singh, R. K., Patil, T., Pandey, D., and Sawarkar, A. N. (2021). Pyrolysis of mustard oil residue: A kinetic and thermodynamic study. _Bioresource Technology_, _339_, 125631. https://doi.org/10.1016/j.biortech.2021.125631

Vejar, A. G., Tolosa, B., Parra, J. W., and Rodríguez-Ordoñez, D. R. (2016). Uso de la cáscara de mamón (_Melicoccus bijugatus_) para el teñido de telas. _Avances en Química_, _11_(3), 123-128. https://www.redalyc.org/articulo.oa?id=93349879004

Vyazovkin, S., Burnham, A. K., Criado, J. M., Pérez-Marqueda, L. A., Popescu, C., and Sbirrazzuoli, N. (2011). ICTAC Kinetics Committee recommendations for performing kinetic computations on thermal analysis data. _Thermochemical Acta_, _520_, 1-19. https://doi.org/10.1016/j.tca.2011.03.034

Wang, C., Wang, X., Jiang, X., Li, F., Lei, Y., and Lin, Q. (2019). The thermal behavior and kinetics of co-combustion between sewage sludge and wheat straw. *Fuel Processing Technology*, *189*, 1-14. https://doi.org/10.1016/j.fuproc.2019.02.024

Yang, H., Ji, G., Clough, P.T., Xu, X., and Zhao, M. (2019). Kinetics of catalytic biomass pyrolysis using Ni-based functional materials. *Fuel Processing Technology*, 195, 106145. https://doi.org/10.1016/j.fuproc.2019.106145

Yuan, X., He, T., Cao, H., and Yuan, Q. (2017). Cattle manure pyrolysis process: kinetic and thermodynamic analysis with isoconversional methods. *Renewable Energy*, *107*, 489-496. https://doi.org/10.1016/j.renene.2017.02.026